CHAPTER- IV

PREPARATION AND CHARACTERISATION OF NIOBIUM OXIDE THIN FILMS

CHAPTER-IV

PREPARATION AND CHARACTERIZATION OF NIOBIUM OXIDE THIN FILMS

4.1 INTRODUCTION

The transition metal oxides form a group of predominantly ionic solids, which exhibit a wide range of optical and electrical properties. Many of these oxides have shown outstanding activity for a variety of electrochemical processes of technological interest. Niobium oxide is one of the versatile oxide materials among the transition metal oxides. Niobium oxide has broad industrial applications especially in optoelectronic technology [1-4]. It is used as cathode in nonaqueous lithium cells [5], aerogels were described by Maurer [6]. Recently, it has been recognised as an electrochromic material [7,8].

Nb_2O_5 thin films/coatings have been made by variety of physical and chemical techniques such as sputtering [9], electron beam evaporation [10], plasma oxidation [11], chemical vapour deposition [12] metallo-organic chemical vapour deposition (MOCVD) [13] and sol-gel process [14]. However, no reports are available in the literature on the preparation of Nb_2O_5 thin films by spray pyrolysis technique (SPT).

A.P.Goswami and A.Goswami prepared niobium oxide films [15] onto the glass substrates, using Nb_2O_5 powder (white) by vacuum evaporation method and studied dielectric and structural properties. Nilgun Ozer et al. prepared niobium oxide films by sol-gel process and magnetron sputtering [16] and compared optical and electrochemical characteristics. Electrical conduction in amorphous Nb_2O_5 oxide films, obtained by electrochemical method (temperature range 293 to 420 K) was studied by G.Jouve [17].

In the present chapter, an emphasis has been given on the deposition of Nb_2O_5 oxide films onto the amorphous glass substrates by pneumatic spray pyrolysis technique, using aqueous solution of Nb as precursor solution and study of their structural, optical and electrical properties. Due to simplicity, low cost and feasibility for mass production, the spray pyrolysis technique has been used.

The niobium oxide films at variable substrate temperature were prepared and the effect of substrate temperature and post annealing treatment on structural, electrical and optical properties was studied using various characterization techniques. Substrate temperature is one of the important parameter, which influences materials properties and can be controlled to obtain desired properties suitable for a particular application.

4.2 Experimental Procedure

Niobium oxide thin films were obtained by spraying a 0.005 M solution of Nb onto preheated amorphous glass substrates. The substrate temperature was varied from 250 to 450°C in the interval of 50°C. The spray rate was kept constant at 8 ml/min. The samples deposited at different substrate temperatures are denoted by N250, N300, N350, N400 and N450, where subscripts denote substrate temperature. The samples were further annealed in air at 500°C for four hours. The annealed samples are denoted by NA250, NA300, NA350, NA400 and NA450 and effect of annealing on above mentioned properties was examined.

Film thickness was determined by using weight difference method. The X-ray diffractometer (Philips PW-1710) with Cuk_α radiation was used for structural

studies in the range of angle 2θ between 10 to 100°. The SEM micrographs were obtained with Cambridge Stereo scan 250-MK3 assembly. Infrared (IR) spectrum was recorded using Perkin-Elmer IR spectrophotometer Model 783 in the spectral range 400 to 4000 cm^{-1}. For IR measurement the pellets were prepared by mixing KBr with niobium oxide powder collected by scratching from the glass substrates in the ratio 300:1 and then pressing the powder between two pieces of polished steel. To determine the band gap energy, optical absorption study was carried out in the wavelength range between 350 to 850 nm, using Hitachi-330 spectrophotometer. DC electrical resistivity measurement was made using a two probe method in the temperature range 300 to 550 K. The thermo-electric force (emf) was measured as a function of temperature in the temperature range of 300 to 475 K.

4.3 Results and Discussion

Standard niobium solution (0.005 M) (the preparation procedure is given in Chapter-III) was sprayed onto preheated amorphous glass substrates through specially designed glass nozzle. The sprayed droplets undergo evaporation, solute condensation and thermal decomposition thereby resulting in the formation of the niobium oxide films. The chemical reaction that may took place is given below.

$$2\,[NbO_4(CHOHCOO^-)_2]^{5-} \xrightarrow[air]{\Delta} Nb_2O_5 + 4H_2O + 8CO_2 \qquad .....4.1$$

The films were found to be uniform and well adherent to the amorphous glass substrates. The colour of film was brownish at lower temperature and changes to slightly grayish at higher temperature. Post annealed films were thin and nearly transparent [27].

4.3.1 Thickness Measurement

Thickness of the films prepared at different substrate temperatures (N250-N450) were measured and the variation is shown in Fig. 4.1(A). The film thickness decreases continuously (from 0.27 μm to 0.06 μm) with increasing substrate temperature from 250 to 450°C. Similar results have been reported for sprayed oxide and chalcogenide films [18,19,20]. This behaviour is attributed to the increase in evaporation rate of initial product before reaching to the substrate, with increasing substrate temperature. Thickness of the post-annealed films were found to be less than that of the as-deposited films (Fig.4.1B). The film thicknesses are listed in Table 4.1

4.3.2 X-ray diffraction (XRD) Studies

The structural identification was carried out using X-ray diffraction in the range of angle 2θ between 10° and 100°. Fig.4.2 shows XRD patterns of niobium

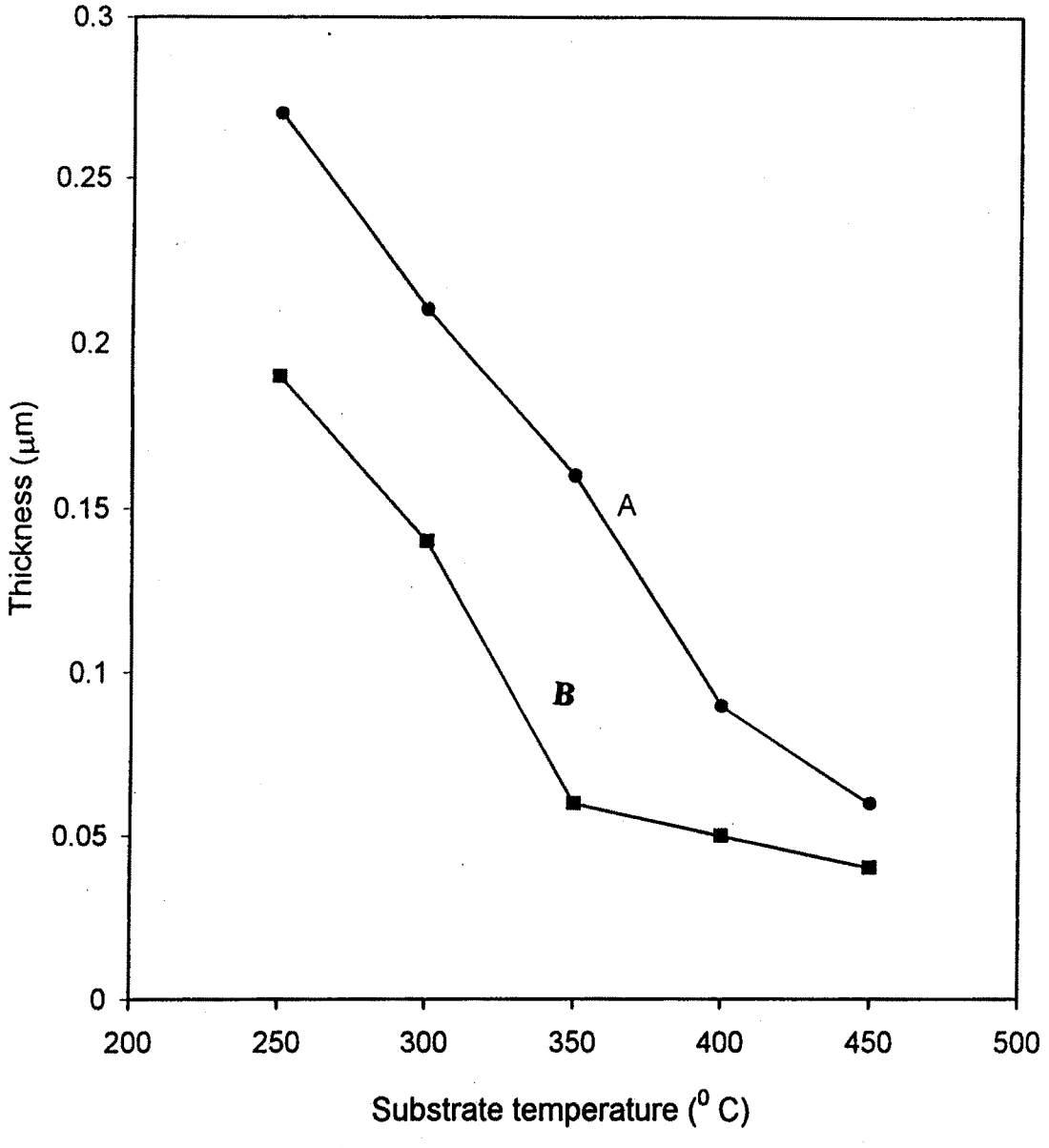

FIG. 4.1: Variation of film thickness with substrate temperature

Table 4.1: Effect of Substrate Temperature on Properties of Niobium Oxide Thin Films Prepared by Spray Pyrolysis

Sample	Thickness (μm)	Grain size (nm)	Bandgap Eg (eV)	Electrical Resistivity At 300 K (Ω -cm)	Activation Energy Eg(eV)	Thermo Electric power(mV/°C)
N250	0.27	-	2.8	3.2×10^{8}	0..84	0.16
N300	0.21	-	2.75	2.0×10^{8}	0.83	0.15
N350	0.16	-	2.7	5.1×10^{7}	0.81	0.08
N400	0.09	-	2.6	3.2×10^{7}	0.79	0.04
N450	0.06	-	2.6	$6..3 \times 10^{6}$	0.78	0.012
NA250	0.19	31	2.6	1.6×10^{8}	0.81	0.80
NA300	0.14	32	2.5	5.0×10^{7}	0.79	0.58
NA350	0.06	35	2.4	1.3×10^{7}	0.78	0.33
NA400	0.05	36	2.35	8.3×10^{6}	0.77	0.16
NA450	0.04	41	2.35	4.7×10^{6}	0.77	0.13

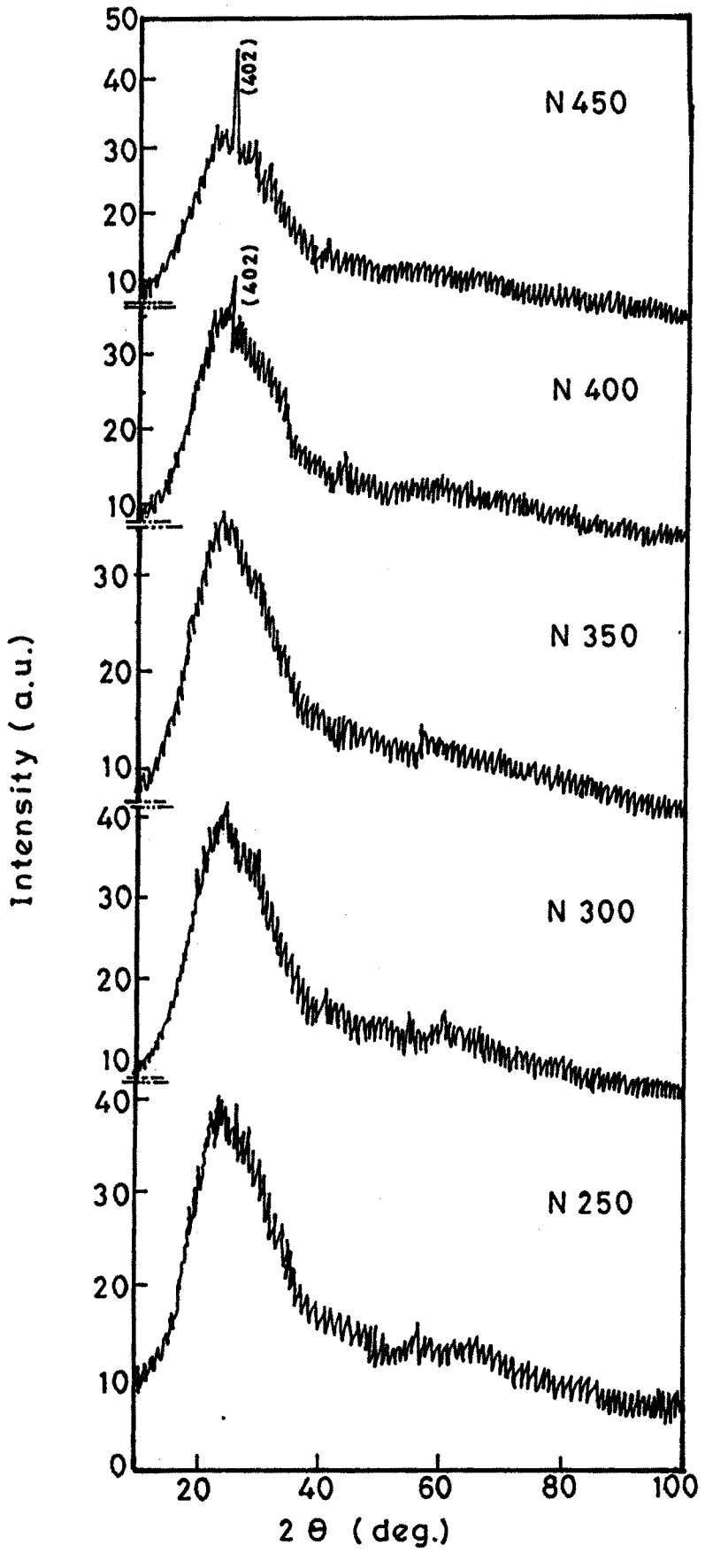

Fig. 4·2 - The XRD patterns of Niobium oxide thin films prepared at different substrate temperatures.

oxide films (samples N250 to N450) prepared at different substrate temperatures. For N250, N300 and N350 samples broad humps can be seen and no well defined peaks were observed. This is the identification of their amorphicity; where as for the samples N400 and N450 some peaks were observed revealing that they are slightly crystalline or microcrystalline with orientation along (402) plane. Similar results have been reported for Nb_2O_5 films prepared by vacuum deposition. Sol-gel and magnetron sputtering methods [15,16]. The 'd 'values of the XRD reflections were compared with standard 'd' values from JCPDS data card (37-1468,43-1042). To diagnose structure and composition of deposited films JCPDS data cards were used. The observed and standard 'd' values are listed in Table 4.2. The good agreement between standard and observed 'd' values suggests that all the samples i.e. N250 to N450 exhibit Nb_2O_5 monoclinic composition.

The samples N250 to N450 were further annealed in air at 500°C for 4 hours. Fig.4.3 shows XRD patterns of annealed films (NA250 to NA450). It is found that all the samples became highly polycrystalline. The films NA250 to NA400 exhibit a major XRD peak corresponding to (-414) plane. Besides a major peak one additional X-ray peak corresponding to (752) plane, which emerges for samples NA350 and NA400 gets ameliorated. This is also a characteristic peak of Nb_2O_5.

The sample NA450 exhibited well defined, high intense diffraction peaks corresponding to ($\bar{2}02$), (220), (211) and (311) planes. The observed and standard

Table 4.2: Comparision between standard and observed 'd' values of as-deposited films

Sample	Angle 2θ	Standard 'd' values (A°)	Observed 'd' values (A°)	I/I_{Max}(%)	Plane (hkl)	Structure
N250	36.02	2.49	2.49	100	(007)	Monoclinic
N300	16.43	5.28	5.38	100	(202)	Monoclinic
N350	77.20	1.23	1.23	100	(208)	Monoclinic
	89.10	1.09	1.09	36	(135)	
N400	25.32	3.48	3.48	100	402	Monoclinic
	40.19	2.28	2.24	12	-108	
N450	25.51	3.48	3.48	100	402	Monoclinic
	31.59	2.82	2.82	9	-414	

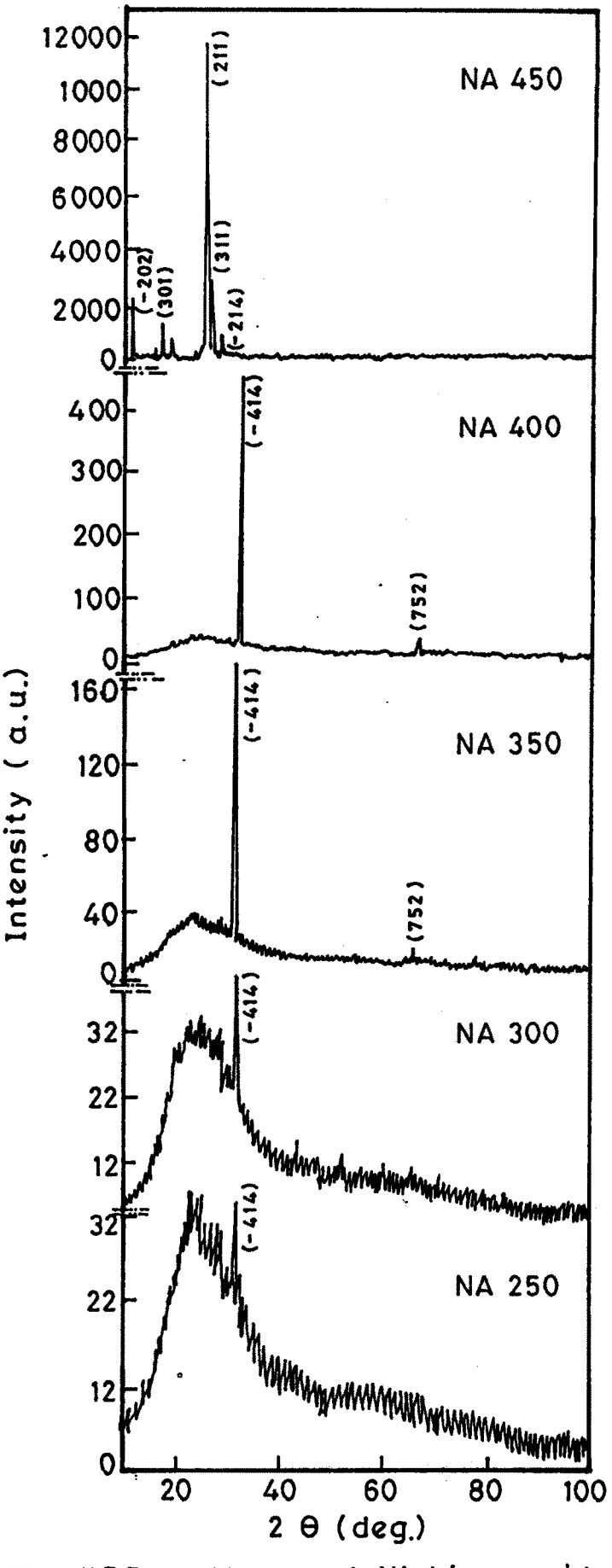

Fig. 4-3 - The XRD patterns of Niobium oxide thin films annealed at 500 °C for 4 hours in air.

'd' values are listed in Table 4.3. The good agreement of observed 'd' values with standard 'd' values from JCPDS data card (37-1468, 43-1043) suggests that all the samples NA250 to NA450 exhibit Nb_2O_5 nomoclinic composition.

In order to determine the grain size, a slow scans of major reflex (along –414 plane for samples NA250 to NA400 and along 211 plane for sample NA450 were carried out with a step of 0.02° min^{-1}. The grain size of the crystallites was calculated using the well-known Scherrers formula, given in Eq. 4.2.

$$D = 0.9\lambda \; / \; \beta \, Cos\theta \qquad .....4.2$$

Where, λ is wavelength (1.5406×10^{-10} m), β is full width in radian at half maximum of the peak and θ is Bragg's angle of the XRD peak. The grain size was found to be varied between 31 to 41 nm for the samples NA_{250} to NA_{450}. The grain size values are listed in Table 4.1.

4.3.3 Scanning Electron Microscopy (SEM)

It is clear from XRD study that as deposited samples N250, N300 and N350 were amorphous, where as samples N400 and N450 were slightly crystalline. Hence it was anticipated that after post annealing treatment samples N400 and N450 exhibit higher crystallinity. To track this, SEM micrograpahs were taken for the annealed samples NA250 to NA450.

Table 4.3: Comparison between standard and observed 'd' values of annealed films

Sample	Angle 2θ	Standard 'd' values (A°)	Observed 'd' values (A°)	I/I_{Max}(%)	Plane (hkl)	Structure
NA250	31.78 33.99	2.82 2.63	2.81 2.63	100 13	(-414) (503)	Monoclinic
NA300	31.78 33.99	2.82 2.63	2.81 2.63	100 30	(-414) (503)	Monoclinic
NA350	31.76 66.24	2.82 1.40	2.81 1.40	100 9	(-414) (752)	Monoclinic + Tetragonal
NA400	31.71 66.24	2.82 1.40	2.81 1.40	100 4	(-414) (752)	Monoclinic + Tetragonal
NA450	10.98 17.35 26.51 27.59 29.60	8.40 5.12 3.35 3.22 3.00	8.04 5.10 3.35 3.22 3.01	19 22 100 24 7	(-202) (301) (211) (311) (-214)	Monoclinic

Fig.4.4 (a-c) shows SEMs of samples NA250, NA300 and NA350 with x 3000 magnification. All these samples were found to have asperity (rough surfaces) and no well-defined grains can be seen. Neverthless sample NA350 exhibit quiet compact structure with uniform distribution of needle shaped fine grains, due to which its resistivity is lowest among amorphous originated samples (NA250, NA300 and NA350) (Table 4.1).

For crystalline originated samples NA400 and NA450 the action of annealing treatment seems to be two fold; Coalescence of fine grains to become appreciably larger and orientation of crystallites. In fig.4.4 (d) for NA400 sample, random orientation of needle shaped grains can be clearly seen. For NA450, fig.4.4 (e), the growth of independent crystallites and their random distribution is visible. Since small grains tend to have surfaces with sharper convexity, they gradually disappears by feeding the larger grains. The net effect is grain growth. Crystallites are found to be larger for NA450 than for NA400 sample, which engenders them relatively higher conductive (4.7×10^6 Ω-cm) than all other samples.

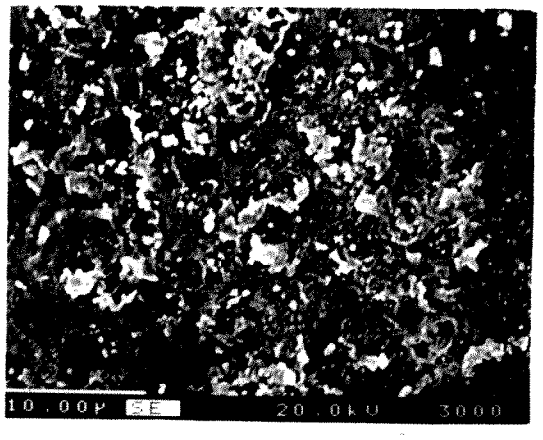

a

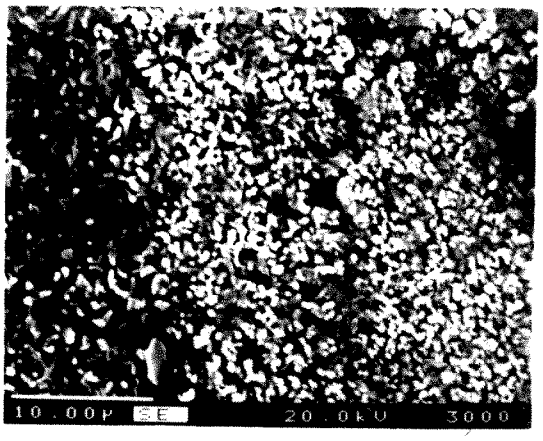

b

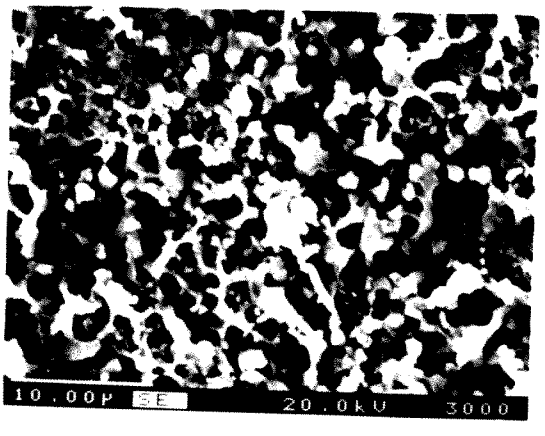

c

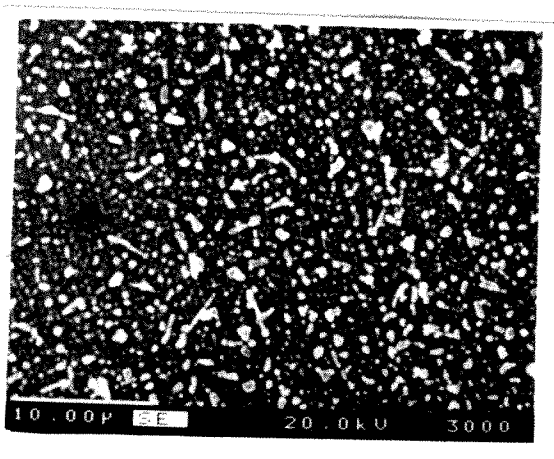

d

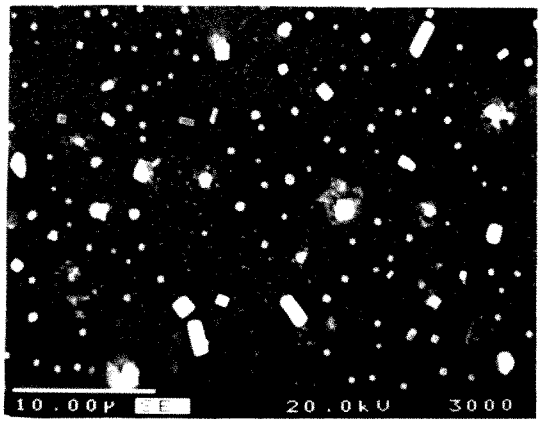

e

Fig.4.4 SEMs of Nb_2O_5 thin films annealed at 500 ^{0}C in air for 4 hours.
a) NA250 b) NA300 c) NA350 d) NA400 e) NA450

4.3.4 Infrared spectroscopy (IR)

Niobium oxide thin film sample was studied by means of IR spectroscopy which gives information about the phase composition and the way in which oxygen is bound to the metal atoms.

IR transmission spectrum of the sample NA350 of niobium oxide thin film, in the wavelength range between 400-4000 cm^{-1} is shown in fig.4.5. The broad absorption at around 3400 cm^{-1} can be assigned to the absorbed water or surface hydration. A water bending vibration produced band at 1560 cm^{-1}.

The IR spectrum displays three distinctive bands. The first band of 560 cm^{-1} is associated with Nb-O stretching. The second band at 710 cm^{-1} is associated with Nb-O-Nb bridging and third band at 860 cm^{-1} is associated with Nb_3O stretching [21,22]. This result confirms the monoclinic structure of Nb_2O_5 thin films.

4.3.5 Optical Absorption Studies

The Nb_2O_5 thin films are optically characterized by measuring the optical density (αt) in the wavelength range of 350 to 850 nm. The values of α were not corrected for the transmittance and the reflectance of the film surface. The absorption coefficient was of the order of $10^4 cm^{-1}$. In order to confirm the nature of the optical transition in these samples, the optical data were analyzed from the classical relation (Eq.3.5) for near edge optical absorption in the semiconductor.

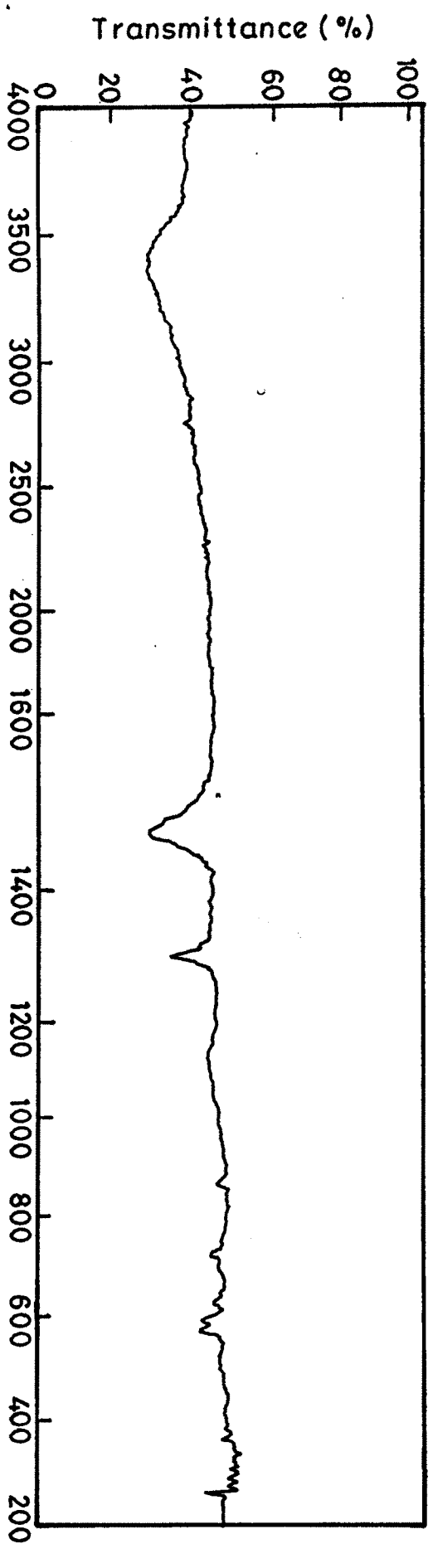

Fig. 4.5 – The IR spectrum of Nb_2O_5 thin film (sample NA 350).

Fig. 4.6 and Fig. 4.7 shows plots of $(\alpha h\nu)^2$ versus $h\nu$ for the samples N250 to N450 and NA250 – NA450 respectively. Linear portion of the $(\alpha h\nu)^2$ versus $h\nu$ plot indicates that optical transition in Nb_2O_5 sample is due to the direct inter-band transition. The optical band gap energy (Eg) values were obtained by extrapolating the straight-line portion of the plot at $\alpha=0$. The Eg values are listed in Table 4.1. It is found that after annealing (crystallization) Eg decreases. Hence it seems that lattice disorder leads to band gap widening, which is analogous to the reported properties for r.f. sputtering Nb_2O_5 films [23].

4.6 Electrical Resistivity

The room temperature electrical resistivity for all the samples were measured and found to vary from 10^8 Ω -cm for thicker samples (N250, N300) to 10^6 Ω-cm for thinner (N450) samples, which is in good agreement with values reported by others [24]. The room temperature electrical resistivity for all the samples are listed in Table 4.1. The values of room temperature electrical resistivity suggest that the films are of Nb_2O_5 excluding the formation of suboxides. For example, $Nb_2O_{4.998}$ has ρ_{RT} of ~ 10^{-1} Ω -cm [25] and NbO_2 has ρ_{RT} of ~10^{-4} Ω -cm [26]. Therefore stoichiometry of sprayed niobium oxide films can be assigned to Nb_2O_5. However, vacuum deposited films invariably associated with the formation of lower oxides different in composition from Nb_2O_5 [27]. The variation of dc electrical resistivity with temperature for these samples in

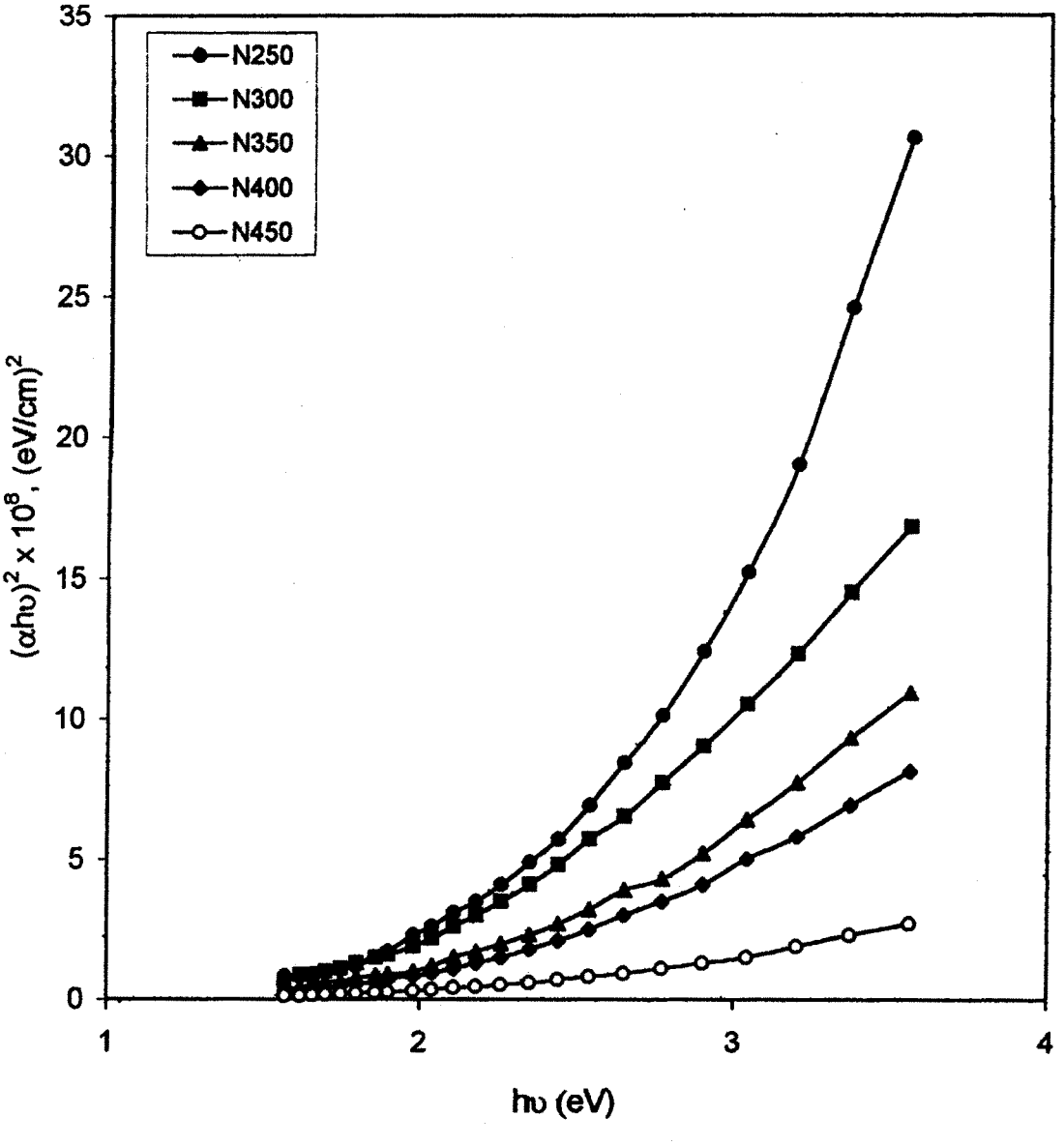

FIG. 4.6: Plot Of $(\alpha h\upsilon)^2$ versus $(h\upsilon)$ for niobium oxide thin films (as deposited)

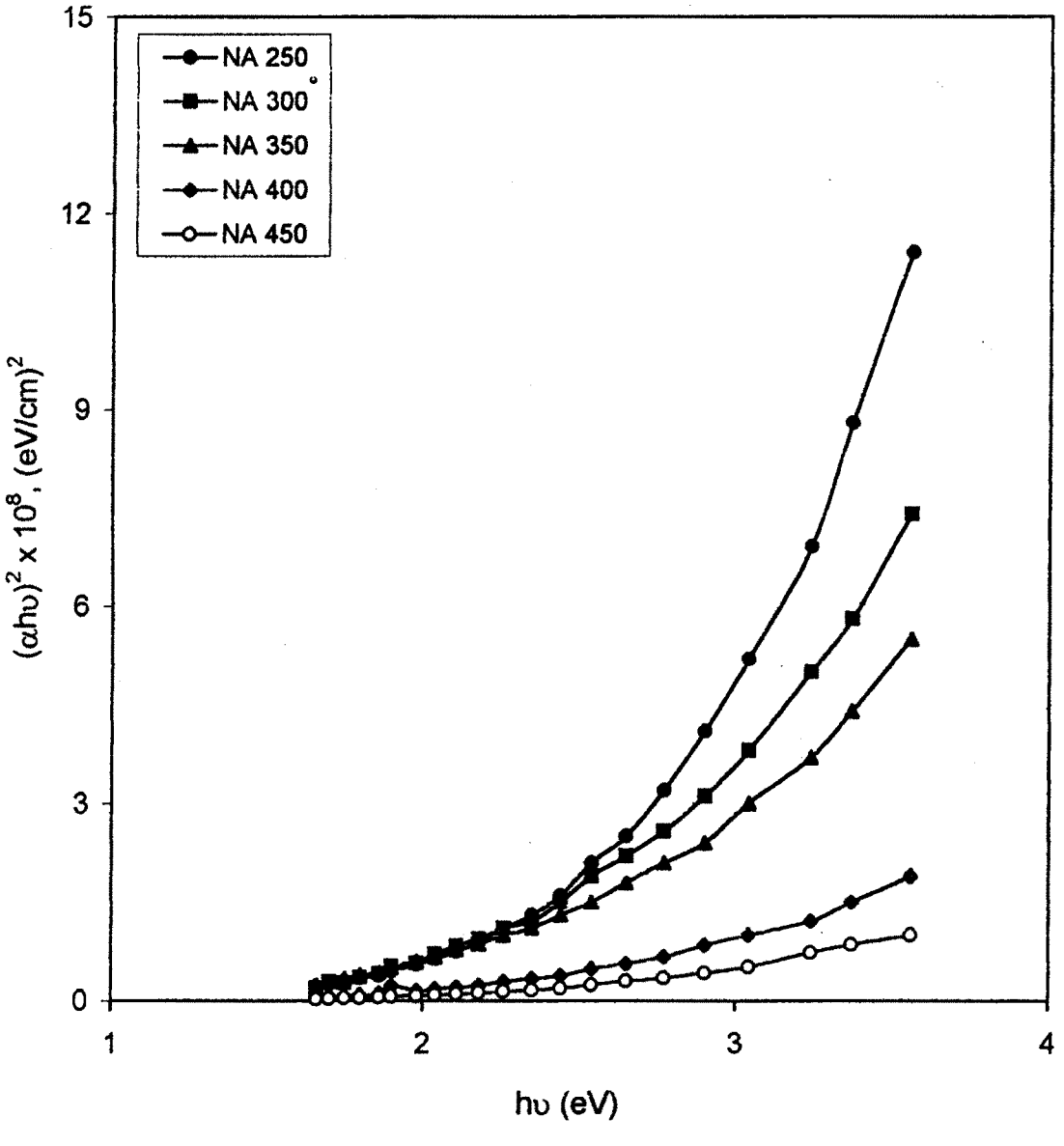

FIG. 4.7: Plot of $(\alpha h\upsilon)^2$ versus $(h\upsilon)$ for niobium oxide thin films (annealed)

the range 300 to 500 K was studied and is shown in Fig. 4.8 and 4.9 for N250 –N450 and Na250-Na450 samples respectively. For all the samples as temperature rises resistivity decreases, indicating that the films are semiconducting in nature.

The thermal activation energy values (Ea) were calculated by using relation (3.4). These values are listed in Table 4.1. In case of oxides, the activation energy is the thermal energy required to hop the charges from one site to other. fig. 4.10 and 4.11 shows the variation of $\log\rho$ versus $(To/T)^{1/4}$ for N250 to N450 and NA250 to NA450 samples respectively. These plots yield straight lines, which suggest that the temperature dependence of electrical resistivity is consistent with the following relation 4.3;

$$\rho = \rho o\, [\, (To/T)^{\alpha}] \qquad \text{.....4.3}$$

where To = 7 X 10^7 K and α depends on kind and degree of disorder of the considered system and on temperature. The result of fig.4.11 and fig.4.12 evinces for variable range hopping of charge carriers between randomly localized electronic states in the system.

4.3.8 Thermo-electric Power Measurement

The temperature dependence causes transport of carriers from hot end to cold end, thus creating an electric field, which gives rise to the thermal voltage. Thermoelectric e.m.f. was measured for Nb_2O_5 films in the temperature range 300 to 475 K. The polarity of the thermally generated voltage at the hot end was

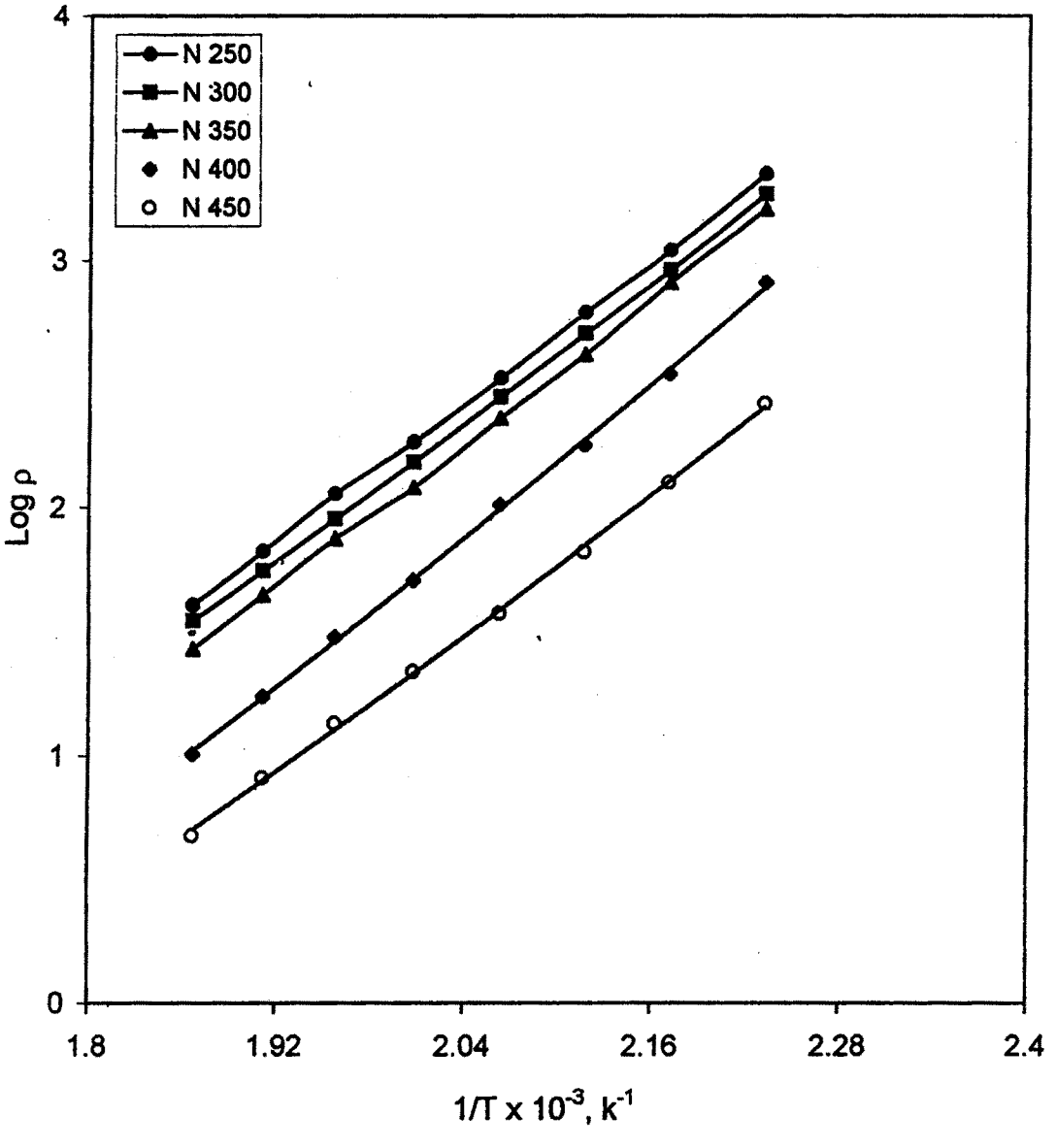

FIG. 4.8: Variation of log ρ versus 1/T for N250-N450 samples

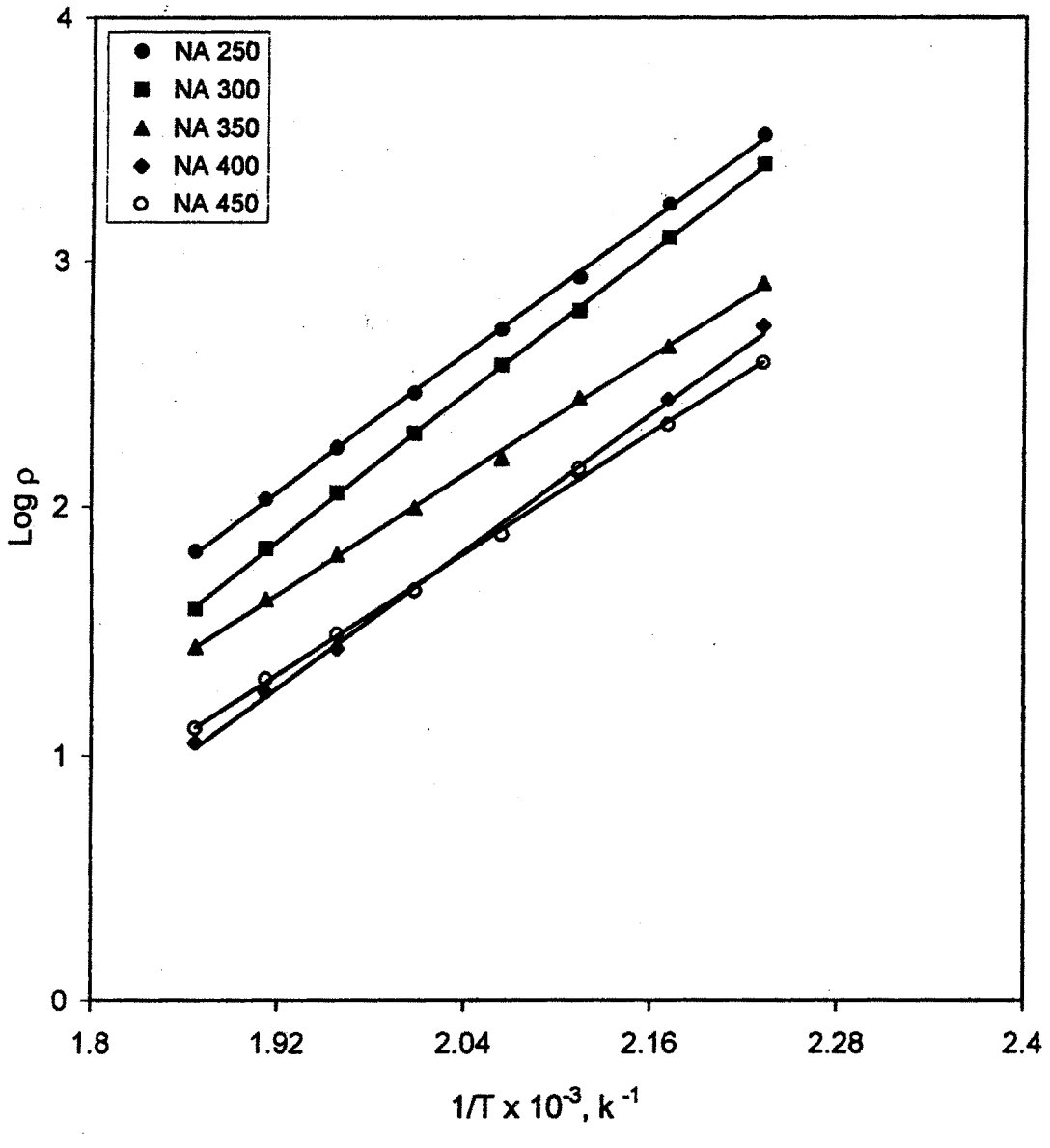

FIG. 4.9: Variation of log ρ versus versus 1/T for NA250-NA450 samples

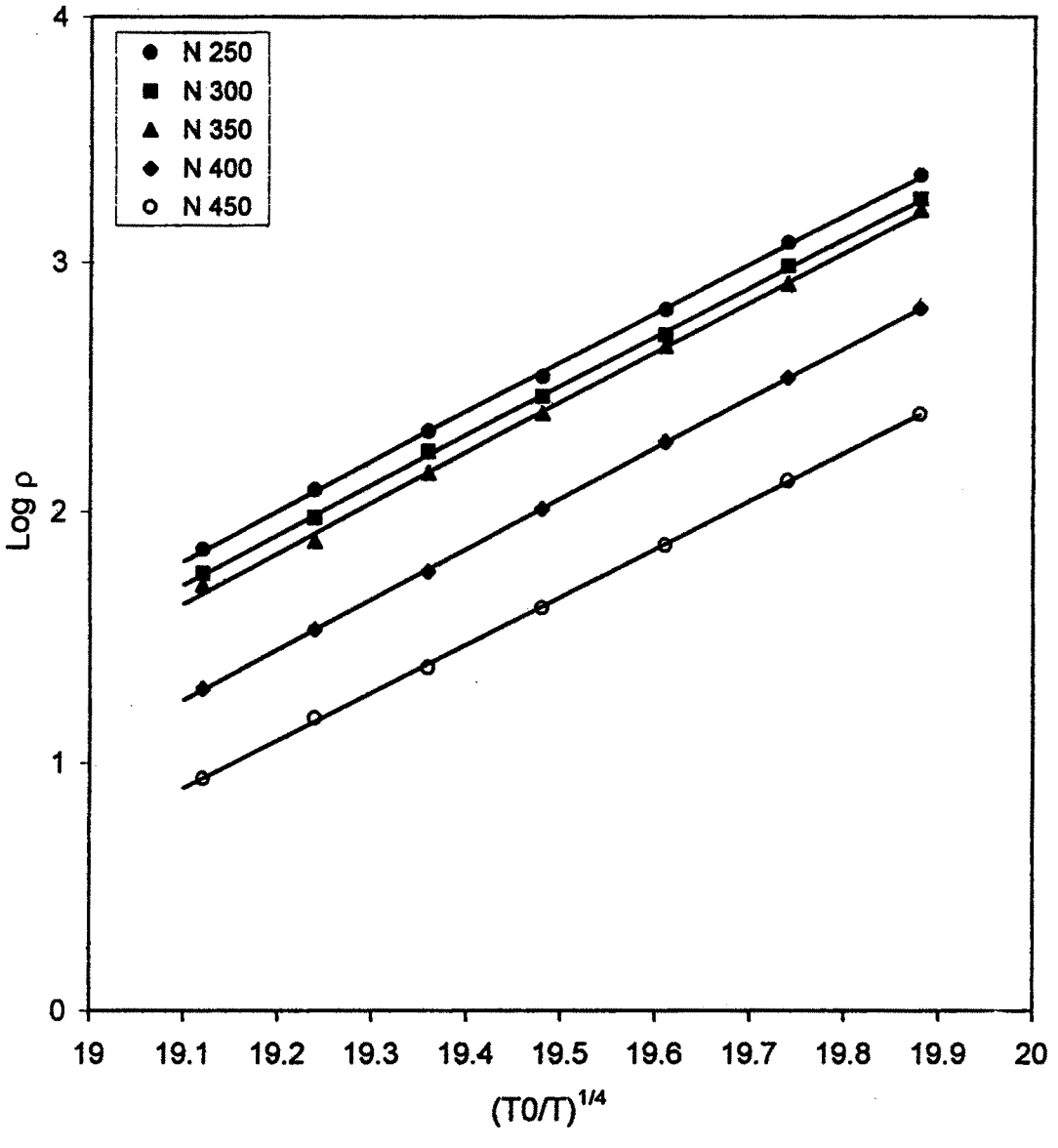

FIG. 4.10: Variation of log ρ versus $(T_0/T)^{1/4}$ for N250-N450 samples

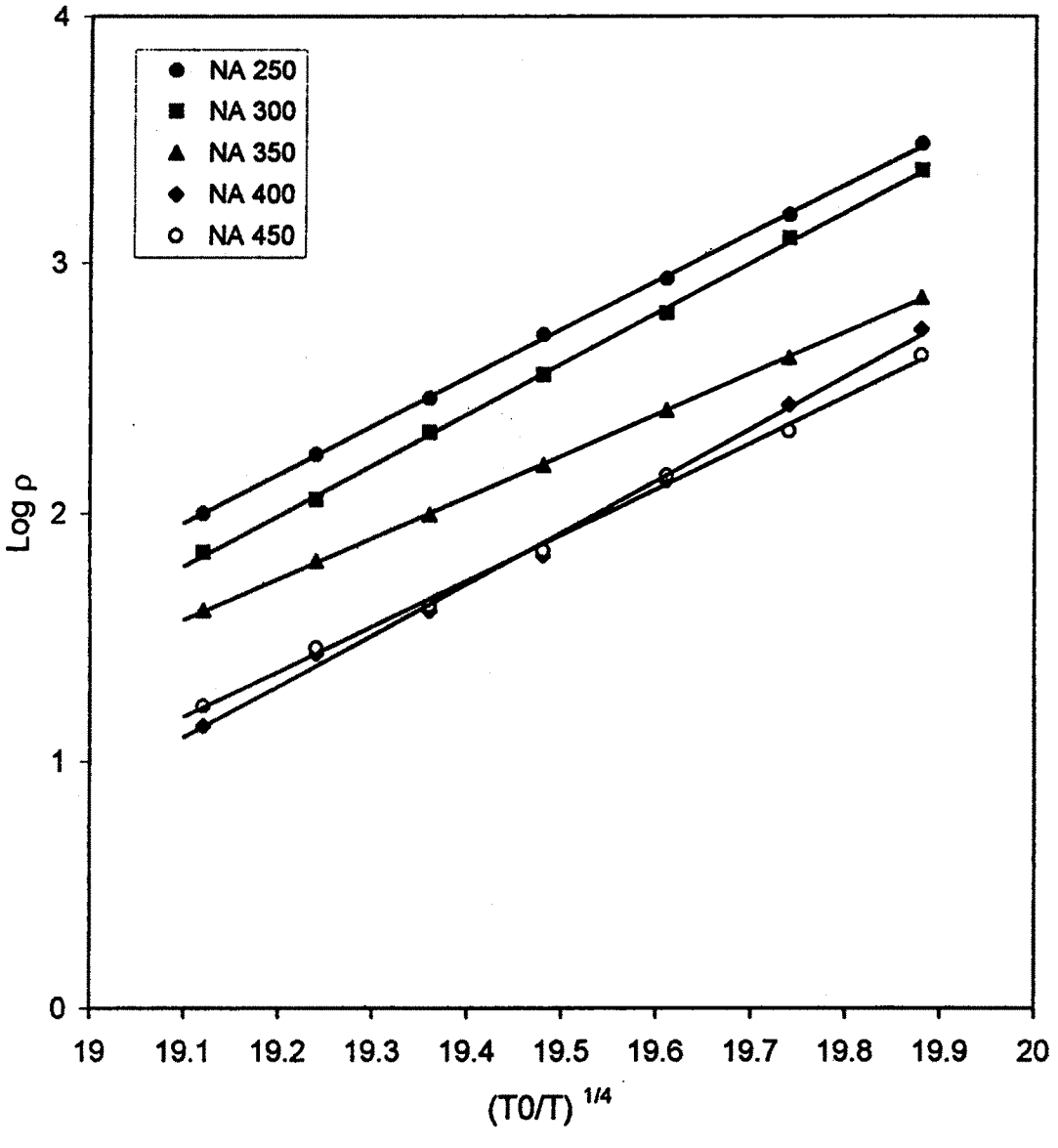

FIG. 4.11: Variation of log ρ versus $(T_0/T)^{1/4}$ for NA250-NA450 samples

positive indicating that the films are N type. G. Jouve reported Nb_2O_5 oxide films, electrochemically performed are of N type [28].

Fig.4.12 and fig. 4.13 shows the variation of thermo-emf with temperature difference for N250-N450 and NA250-NA450 samples respectively. The thermo-emf increases non-linearly with increase in temperature difference. This may be attributed to increase in the mobility of charge carrier and carrier concentration with rise in temperature.

The observed values of thermo-emf for samples N250 and NA250 were largest, and these values were smallest for samples N450 and NA450. The thermoelectric power for all the samples was calculated by fitting the exponential curve to the experimental data and are listed in Table 4.1.

4.4 Conclusions

Niobium oxide thin films were deposited onto the amorphous glass substrates at various substrate temperatures from 250 to 450°C in the interval of 50°C, using spray pyrolysis technique. The film thickness decreases from 0.27 to 0.06 μm as substrate temperature varied from 250 to 450°C. XRD studies showed that the films deposited at 250,300 and 350°C are amorphous, while the films deposited at 400 and 450°C show slight crystallinity. The optical absorption analysis suggested the presence of direct inter-band transitions. The optical band gap energy decreases with increase in substrate temperature. The room temperature electrical resistivity varies from 3.2 X 10^8 to 6.3 X 10^6 Ω -cm with

increase in substrate temperature from 250 to 450°C, showing n type semiconductivity.

An interesting result was obtained, when films are annealed at 500°C for 4 hours. XRD and IR studies showed that the annealed films were polycrystalline consisting Nb_2O_5 monoclinic phase. Thickness, electrical resistivity and band gap of the annealed films were decreased. Therefore, it is concluded that the material properties can be tailored merely by changing the substrate temperature.

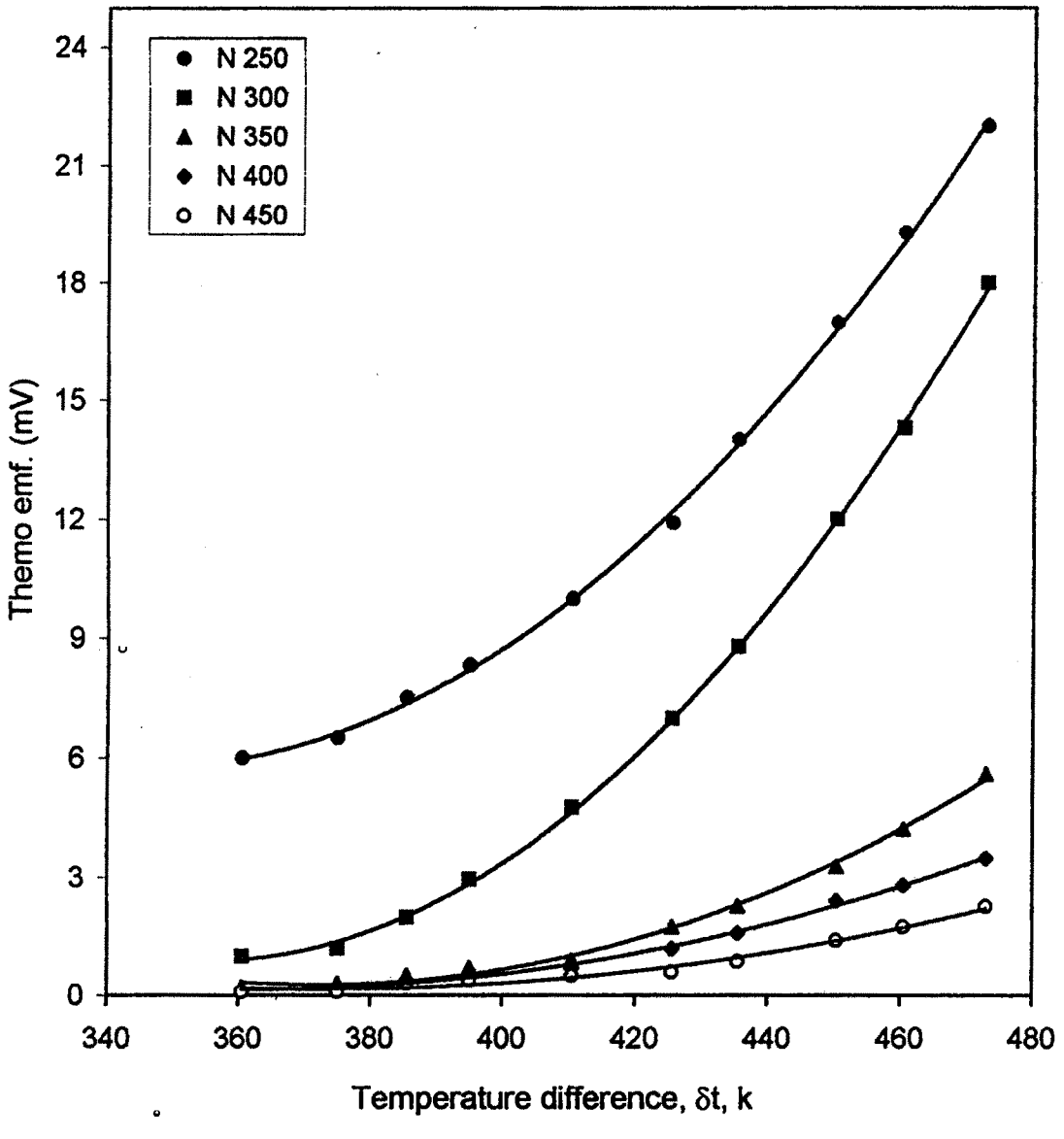

FIG. 4.12: Variation of thermo emf with temperature difference for N250-N450 samples

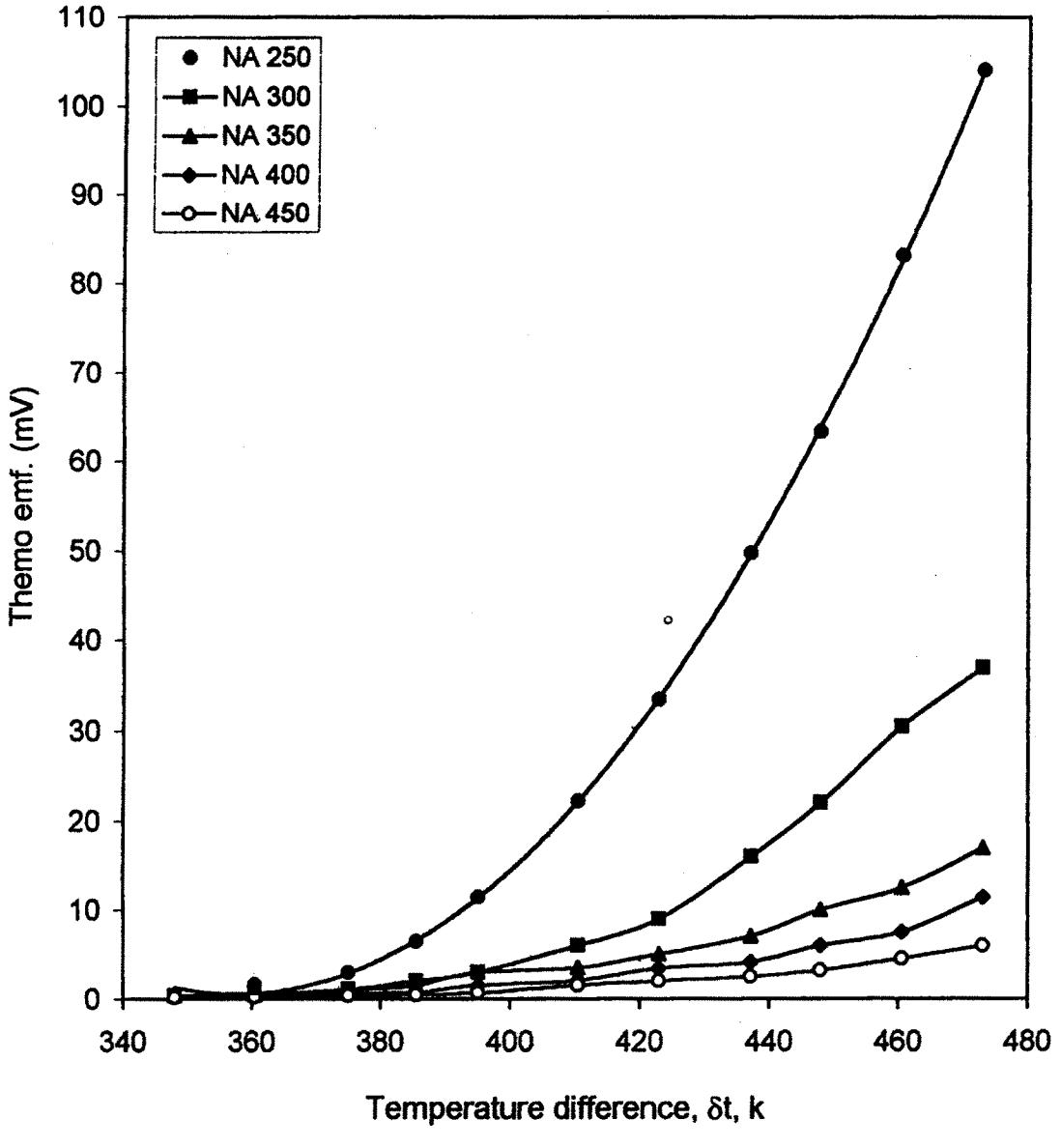

FIG. 4.13: Variation of thermo emf with temperature difference for NA250-NA450 samples

REFERENCES

1 S.K.Deb. Solar Energy Mater. 25 (1992) 327

2 C.G. Granqvist, Solid State Ionics 53-56 (1992) 479

3 R.B. Goldner, F.O. Amtz, G.Berera, T.E. Hass, G.Wei, K.K. Wong and P.C., Yu. Solid State Ionics 53-56 (1992) 617.

4 N.Ozer, T.Barreto, T. Buyuklimanli and C.M. Lampert, Sol. Energy Mater. Sol.Cells 36 (1995) 433.

5 B.Reichman and A.J.Bard, J.Electrochem. Soc. (1980) 344-346

6 Maurer S.M., D.Ng. and E.I.Ko, Catal. Today 16, 319-331 (1993)

7 M.Macels, B.Orel. Solar Energy Mater, and Solar Cells 54 (1998) 121-130

8 M.Schmitt, S.Heusing, M.A. Aegerter, A.Pawlicka, C.Avellaneda. Solar energy Mater. And Solar Cells 54 (1998) 9-17

9 R.Cabanel, J. Chaussy, J.Mazuer. G. Delabouglise, J.C. Joubert, G.Barral and C.Montella. J. Electro Chem. Soc. 137 (1996) 1444

10 D.K. Benson and C.E. Tracy, Chemtech. November (1991) 677

11 J.G. Zhang, C.E. Tracy, D.K. Benson and S.K.Deb, J.Mater. Res. 8 (1933) 2649

12 C.G. Granqvist, Solid State Ionics 53-56 (1992) 479 / Repeated Ref 2

13 N.Hara, E. Takahashi, J.H. Yoon and K.Sugimoto, J.electrochem. Soc. Ionics 141 (1994) 1669

14 G.R.Lee and J.A. Crayston, J.Mater.Chem 1 (1991) 381

15 Amit P. Goswami and A Goswami. Indian Journal of Pure and Applied Phy. 12 Jan. 1974 PP. 26-31

16 Nil gun Ozer, Michael D.Rubin, Carl M.Lampert. Solar energy Materials and Solar Cells 40 (1996) 285-296

17 G.Jouve, Philosophical Magazine B 1991 Vol.64 No.2 207-218

18 L.W.Chow, Y.C.Lei and H.L. Lwok, Thin Solid Films, 81 (1981) 3706

19 M.D.Uplane and S.H.Pawar, Solid State Comm. 46 (1983) 847

20 S.H.Pawar,S.P. Tamhankar and C.D.Lokhande, J.Matt. Sci. Lett. 3 (1984) 427

21 T. Ikeya, M.Senna, J.Non-Cryst-Sol 105 (1988) 243

22 M.Macek, B.Orel, Solar Energy Materials and Solar Cells 54 (1998) 121-130

23 T.Maruyama and S.Arai, Solar Energy Mater, and Solar Cells 30 (1993) 257

24 T.Hyoid, E.Kanazawa, Y. Takao, Y.Shimizu and M. Egashiva, Electrochemistry, 68 (2000) 24

25 R.F. Janinck and D.H. Whitmore, J.Chem. Phys., 37 (1962) 2750

26 J.A. Roberson and R.A. Rapp, J.Phys. Chem. Sol., 30 (1969) 1119

27 A.Goswami and A.P. Goswami, Ind.J.Pure and App.Phys., 13 (1975) 667

28 Jouve, G., 1990, C.R. Acad. Sci., Paris, 311, Serie II, 929.